

Concept Guided Co-saliency Object Detection

Jiayi Zhu¹, Qing Guo³, Felix Juefei-Xu², Yihao Huang⁴, Yang Liu⁴, Geguang Pu^{1,5}

¹ East China Normal University, China ² New York University, USA

³ IHPC & CFAR, Agency for Science, Technology and Research, Singapore

⁴ Nanyang Technological University, Singapore

⁵ Shanghai Industrial Control Safety Innovation Tech. Co., Ltd, China

Abstract

The task of co-saliency object detection (Co-SOD) seeks to identify common, salient objects across a collection of images by examining shared visual features. However, traditional Co-SOD methods often encounter limitations when faced with diverse object variations (e.g., different postures) and irrelevant background elements that introduce noise. To address these challenges, we propose ConceptCoSOD, a novel concept-guided approach that leverages text semantic information to enhance Co-SOD performance by guiding the model to focus on consistent object features. Through rethinking Co-SOD as an (image-text)-to-image task instead of an image-to-image task, ConceptCoSOD first captures shared semantic concepts within an image group and then uses them as guidance for precise object segmentation in complex scenarios. Experimental results on three benchmark datasets and six corruptions reveal that ConceptCoSOD significantly improves detection accuracy, especially in challenging settings with considerable background distractions and object variability.

1. Introduction

Co-salient object detection (Co-SOD) plays a crucial role in numerous computer vision applications, including data preprocessing for weakly supervised semantic segmentation [43] and video object localization [21, 22]. The goal of Co-SOD is to detect common and prominent objects by analyzing the intrinsic relationships within related image groups. This task demands the simultaneous processing of multiple images to extract and align shared features, presenting considerable challenges due to the substantial variation in object appearance, orientation, and background across different scenes.

Previous research has addressed the Co-SOD problem from multiple perspectives. Early studies [3, 10, 27] relied

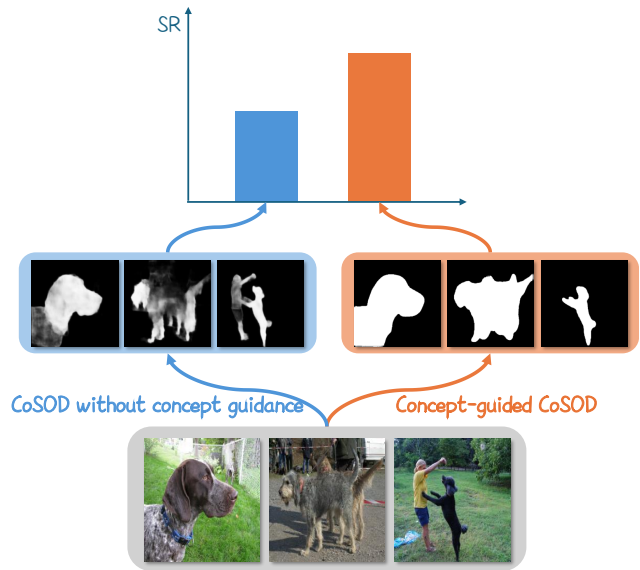


Figure 1. Co-saliency object detection results w/o the concept guidance.

on manually selected features, such as color and texture, to identify consistency across related image groups. However, these handcrafted shallow features are limited in robustness and practicality. Consequently, learning-based methods have diversified, incorporating deep learning [26, 39], self-paced learning [17, 46], metric learning [14], and graph-based learning [23, 53] to explore semantic relationships within image groups, achieving substantial advancements. However, two primary challenges remain. The first is *inter-object variations*, where attributes such as posture vary within the same category (e.g., “dogs”). The second is *background distractions*, where unrelated elements, like occasional “human” in the background, introduce visual noise. Effective Co-SOD methods must address these challenges by mitigating the influence of both inter-object variations and background distractions.

With the growing popularity and effectiveness of vision-language methods in segmentation tasks [2, 29, 30, 40, 41],

it is worth exploring whether this text-driven approach (*i.e.*, leveraging text semantics for vision tasks) could be adapted to the Co-SOD task. In our opinion, the text-driven approach offers two advantages for addressing the main challenges in the Co-SOD task: ❶ Condensed semantic information in the text (*e.g.*, semantic of “dog”) reduces the impact of subtle variations within the same category, such as posture differences, enabling more precise segmentation of target object regions against *inter-object variations*. ❷ Under varying visual conditions (*e.g.*, lighting, or background clutter), language provides consistent semantic guidance, allowing the model to focus on the target object despite visual noise from unrelated elements like “human” in the background, thereby enhancing segmentation accuracy and robustness against *background distractions*.

To this end, instead of treating Co-SOD as a traditional image-to-image task, we propose rethinking it as an (image-text)-to-image task by incorporating text semantics as additional information. Specifically, our method comprises two key modules: ❶ For a given image group containing the same target object, we first extract text-based semantic information of the target object (*i.e.*, concept) related to the target object within the images. These concepts are robust, capturing real-world diversity, including variations in perspective, appearance, and object positioning. ❷ We then leverage these learned concepts to achieve fine-grained segmentation of the target object. We introduce this end-to-end concept-guided co-saliency object detection method as *ConceptCoSOD*. Fig. 1 illustrates an example of the *ConceptCoSOD* comparing with traditional co-saliency object detection methods. As shown, traditional co-saliency object detection methods lacking concept guidance produce suboptimal results. In contrast, our concept-guided *ConceptCoSOD* achieves highly accurate detections on public datasets compared to state-of-the-art methods.

Our main contributions are summarized as follows:

- To the best of our knowledge, we present the first concept-guided co-saliency object detection method. By fully leveraging text semantics extracted from the input image group as supplementary information, instead of treating Co-SOD as a traditional image-to-image task, we propose rethinking it as an (image-text)-to-image task.
- We design a novel pipeline consisting of two modules: the concept learning module, which extracts concrete text semantic information, and the concept-guided segmentation module, which leverages the text semantic information to perform fine-grained segmentation directly.
- Extensive experiments were conducted on three benchmark clean datasets and four datasets with different types of corruptions, confirming the **effectiveness** and **robustness** of the proposed *ConceptCoSOD* method.

2. Related Work

2.1. Co-salient Object Detection

Co-Saliency Detection (Co-SOD) focuses on identifying shared, prominent objects by examining the intrinsic relationships among a group of related images [36, 49]. Traditional Co-SOD techniques [21, 28, 34] relied on hand-crafted cues or superpixel-based strategies to capture co-salient areas. However, these manually designed, shallow features often suffer from limitations, proving rigid and insufficient for complex scenarios. With advancements in deep learning, more sophisticated, data-driven Co-SOD approaches have emerged [9, 51], utilizing deeper feature representations to achieve robust consensus formation and feature distribution. These methods first aggregate features from all images in a group to establish a consensus representation, which is then distributed back to the individual image features, enhancing co-saliency extraction. For example, Wang et al. [38] used feature aggregation via summation and applied a gradient feedback mechanism to redistribute the consensus. Jin et al. [24] introduced IC-Net, utilizing a set of enhanced intra-saliency vectors and a dense correlation module for precise distribution. Zhang et al. [51] proposed GICD which employs a gradient-induced mechanism that pays more attention to discriminative convolutional kernels that help to locate the co-salient regions. Zhang et al. [48] presented an adaptive graph convolutional network (GCAGC) with attention graph clustering for co-saliency detection. Fan et al. [9] constructed a consensus attention map through an affinity module, which they multiplied back to the individual image features in the proposed method GCoNet. Zhang et al. [50] proposed CADC, encoding consensus information using dynamic kernels and convolving them with image features to effectively distribute consensus knowledge across the group, enhancing overall saliency detection accuracy. Yu et al. [42] introduced a framework called DCFM for mining comprehensive and democratically shared co-salient features without relying on additional information, enhancing detection accuracy.

2.2. Text-to-Image Diffusion Generation Model

Text-to-image (T2I) generation [44], popularized by diffusion models [4, 16, 31] are highly effective at generating diverse and realistic images based on user-specified text prompts, raising various applications [20]. The development of this approach began with Ho *et al.* introducing a new generation paradigm, denoising diffusion probabilistic models (DDPMs) [16], which demonstrated competitive performance compared to the widely recognized PG-GAN [25]. Recently, the latent diffusion model (LDM) [31] was proposed to perform denoising in latent space, followed by decoding into detailed images, thereby significantly enhancing generation speed and reducing computational com-

plexity. The popular text-to-image model Stable Diffusion [35] is built on LDM.

2.3. Concept Learning

In concept learning (*i.e.*, personalization) tasks, users provide a few image examples of a desired concept, which are then used to generate novel scenes featuring these newly introduced concepts through text prompts. Current personalization methods typically follow one of two approaches: encapsulating a concept via a word embedding at the input of the text encoder [5, 11], or fine-tuning the weights of diffusion-based modules through various techniques [12, 18, 19, 32, 33]. In our method, we leverage the semantic extraction capability of personalization techniques to capture shared semantics across the image group.

3. Preliminaries

3.1. Problem Formulation

Given a group of images $\mathcal{I} = \{\mathbf{I}_i \in \mathbb{R}^{H \times W \times 3}\}_{i=1}^N$ containing N images that have common salient objects, the co-saliency object detection (Co-SOD) task is to detect and segment all common salient objects present within the image group. We denote a Co-SOD method as $\text{CoSOD}(\cdot)$ and predict N saliency maps via

$$\mathcal{S} = \{\mathbf{S}_i\}_{i=1}^N = \text{CoSOD}(\mathcal{I}), \quad (1)$$

where $\mathbf{S}_i \in \mathbb{R}^{H \times W}$ is a binary saliency map corresponding to the salient region of \mathbf{I}_i .

3.2. Motivation

Through an investigation of existing Co-SOD methods, we identify two primary challenges.

Inter-object variations. The first challenge arises from significant variations in the shape of the common salient object across different images within the same group. Factors such as posture and viewing angle can lead to inaccurate Co-SOD predictions. For example, in the first row of Fig. 2, the “guitar” is shown from an unusual bottom-up perspective, which causes current state-of-the-art (SOTA) methods to struggle to produce accurate detection results.

Background distractions. The second challenge involves background distractions in group images, which can mislead Co-SOD methods into detecting incorrect objects. As shown in the second row of Fig. 2, the target co-saliency object is the “eggplant” in the bottom left corner of the image. However, existing methods mistakenly shift focus to non-target objects due to these distractions.

To address these two challenges, our high-level idea comes from the effective practice of vision-language methods in segmentation tasks [2, 29, 40, 41], which exploit text semantic as valuable supplementary information to improve

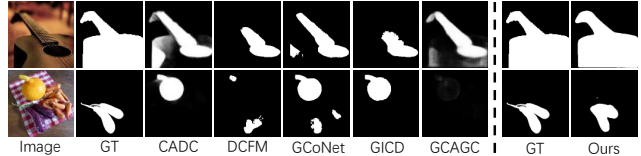


Figure 2. Problem of existing Co-SOD methods.

the performance of the task. To be specific, ❶ The condensed semantic information in text minimizes the influence of subtle variations within the same category, such as differences in posture, enabling more accurate segmentation of target object regions amidst *inter-object variations*. ❷ Under diverse visual conditions (e.g., lighting, or background clutter), language offers consistent semantic guidance, directing the model’s focus toward the target object while mitigating visual noise from unrelated elements, thereby improving segmentation accuracy and robustness against *background distractions*.

Although leveraging text semantics for the Co-SOD task is promising, no textual information is directly available within the task. Hence, we propose to extract effective semantic information directly from the group of images first and then utilize it to guide subsequent detection. By rethinking the Co-SOD task from an image-to-image to an (image-text)-to-image paradigm, we reformulate the method from Eq. (1) to a new one as follows:

$$\mathcal{S} = \{\mathbf{S}_i\}_{i=1}^N = \text{CoSOD}(\mathcal{I}, \text{Extract}(\mathcal{I})), \quad (2)$$

where $\text{Extract}(\cdot)$ denotes the text semantic extraction.

With this design, our approach effectively overcomes the two challenges faced by previous Co-SOD methods in handling difficult scenarios. As shown on the right panel of Fig. 2, our method accurately identifies the correct target object and produces reliable Co-SOD results, regardless of uncommon viewing angles or the presence of distracting background elements.

4. Methodology: CONCEPTCOSOD

4.1. Overview

We propose a method termed *ConceptCoSOD*, which comprises two modules. The first module $\text{ConceptLearn}(\cdot)$ involves utilizing a group of input images for learning the text embedding (*i.e.*, concept \mathbf{c}^*) of the co-existing object in the image group \mathcal{I} :

$$\mathbf{c}^* = \text{ConceptLearn}(\mathcal{I}), \quad (3)$$

The second module $\text{SOD}(\cdot)$ uses the learned concept as guidance to generate co-saliency object detection results through an end-to-end approach. Specifically, the learned concept is applied to perform object detection on each image \mathbf{I} in the image group \mathcal{I} :

$$\mathbf{S}_i = \text{SOD}(\mathbf{c}^*, \mathbf{I}_i), \mathbf{I}_i \in \mathcal{I}. \quad (4)$$

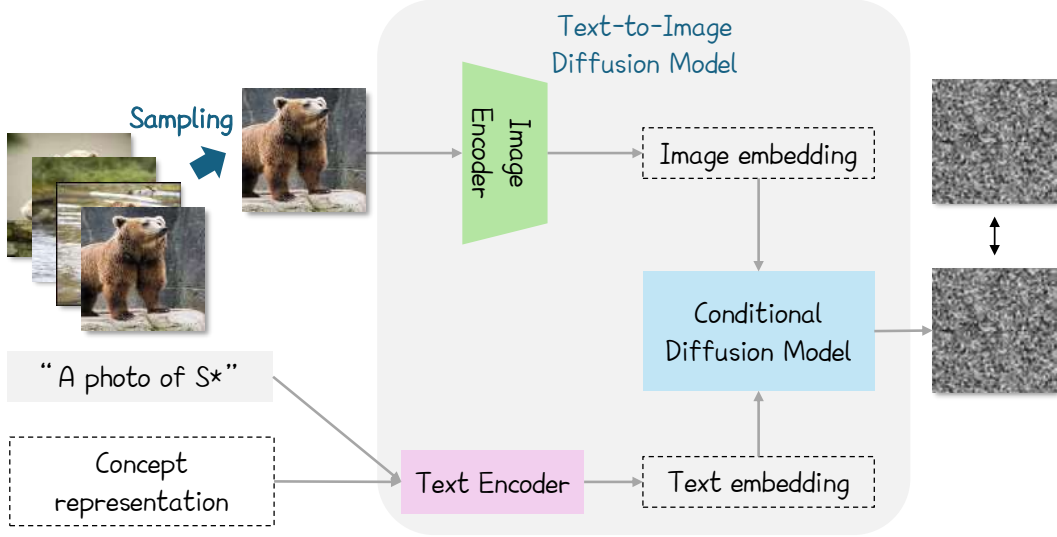


Figure 3. Group-Image concept learning module.

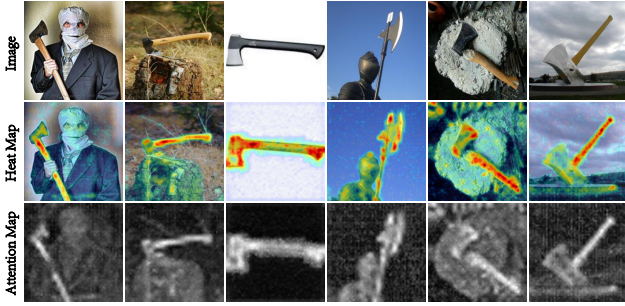


Figure 4. Visualization of the relationship between the concept learned by our method with image group.

The detailed explanation of the two modules is demonstrated in Sec. 4.2 and Sec. 4.3.

4.2. Group-Image Concept Learning

This module aims to learn the text semantic information (*i.e.*, concept) \mathbf{c}^* from the image group \mathcal{I} . Drawing inspiration from the semantic extraction capabilities of personalization techniques [11] which can generate images of a specific object in diverse scenes using only a few photos of that object, we adopt this approach to capture the concept of the target object from the image group. Note that the concept \mathbf{c}^* , learned by the `ConceptLearn(\cdot)` module, represents a token in the latent space of the diffusion model, encapsulating the semantic information of the co-existing object within the image group. The architecture of this module is as below and shown in Fig. 3.

Architecture of text-to-image diffusion model. We utilize a classic text-to-image diffusion model [31] to search for the concepts we need to learn. The text-to-image dif-

fusion model consists of three core modules: (1) an image autoencoder, (2) a text encoder, and (3) a conditional diffusion model. The image autoencoder module comprises an encoder \mathcal{E} and a decoder \mathcal{D} . The encoder maps the input image \mathbf{X} to a low-dimensional latent space $\mathbf{z} = \mathcal{E}(\mathbf{X})$, while the decoder converts the latent representation back to the image space $\mathcal{D}(\mathcal{E}(\mathbf{X})) \approx \mathbf{X}$. The text encoder Γ first tokenizes the text \mathbf{y} and then translates the tokenized results into text representations in the latent space, $\Gamma(\mathbf{y})$. The input to the conditional diffusion model ϵ_θ consists of the time step t , the noise latent variable at step t , \mathbf{z}_t , and the text representation $\Gamma(\mathbf{y})$. This conditional diffusion model can predict the noise added to \mathbf{z}_t at time step t , denoted as $\epsilon_\theta(\mathbf{z}_t, t, \Gamma(\mathbf{y}))$.

Given the image group \mathcal{I} and the pretrained text-to-image diffusion model, we aspire to learn a concept of \mathcal{I} via the following optimization:

$$\mathbf{c}^* = \arg \min_{\mathbf{c}} \mathbb{E}_{\mathbf{z}, \mathbf{y}, \epsilon \in \mathcal{N}(0,1), t \sim \mathcal{U}([0,1])} (\|\epsilon_\theta(\mathbf{z}_t, t, \Phi(\Gamma(\mathbf{y}), \mathbf{c})) - \epsilon\|_2^2), \quad (5)$$

where \mathbf{y} is a fixed text (*i.e.*, ‘a photo of S^* ’), and the function $\Phi(\Gamma(\mathbf{y}), \mathbf{c})$ represents an injection process that replaces the ‘ S^* ’ token in $\Gamma(\mathbf{y})$ with the learnable embedding \mathbf{c} . During the optimization process of this formula, the concept \mathbf{c} is iteratively optimized such that the noise predicted by the diffusion model gradually approaches the ground truth noise ϵ . The Eq. (5) forces the optimized concept \mathbf{c}^* to represent the position of the co-salient objects in the image group within the text latent space. After obtaining \mathbf{c}^* , we can embed the ‘ S^* ’ token into other texts and generate new images using the text-to-image diffusion model.

To verify the effectiveness of the concepts, we visualize

the concept within the image group in Fig. 4. The results demonstrate that the learned concept is closely aligned with the target object (*i.e.*, axe).

4.3. Concept-Guided Segmentation

4.3.1 Preliminary Exploration

To investigate whether the learned concept \mathbf{c}^* can be applied to the co-saliency object detection task, we leverage the well-known interpretability method DAAM [37] for a preliminary exploration. DAAM is designed to interpret the internal mechanisms of large-scale text-to-image models. For a given text input and a text-to-image model, DAAM analyzes the associations between individual words in the text and specific elements within the generated image, visualizing how input text prompts influence different regions of the image. It is implemented by exploiting the attention block (containing a self-attention layer and a cross-attention layer) in the UNet portion of the conditional text-to-image model. Specifically, DAAM uses the text representation and latent representation (*i.e.*, the image embedding) as input, extracting the output features (*i.e.*, attention maps) of the cross-attention layer to illustrate the relationships between the latent image representation and the text representation.

Given the DAAM method as a function $\text{AttnExtract}(\cdot)$, We exploit the optimized concept learned from the image set as \mathbf{c}^* , and the process of extracting features from the cross-attention layer is represented as:

$$\mathbf{f}_{attn} = \text{AttnExtract}(\epsilon_\theta, \mathbf{z}_t, t, \mathbf{c}^*), \quad (6)$$

where \mathbf{z}_t represents the latent representation corresponding to the image at time step t , ϵ_θ denotes the parameters of the text-to-image model, and \mathbf{f}_{attn} refers to the association features (a set of attention maps) that we extract from the selected cross-attention layers. To obtain the final attention map \mathbf{S} , we apply average operation on the \mathbf{f}_{attn} :

$$\mathbf{S} = \text{Avg}(\mathbf{f}_{attn}). \quad (7)$$

Fig. 4 demonstrates the effectiveness of DAAM in segmenting the co-salient object. The first row shows images with an axe as the target co-salient object. The second row overlays the predicted co-saliency detection results as heatmaps on the original images for a clearer, more intuitive visualization. The third row presents the final co-saliency object detection results obtained using DAAM. It can be observed that DAAM demonstrates the potential for co-saliency detection, but the visualization results lack precision. Specifically, while the contours of the target axe are discernible in the predicted grayscale images, the segmentation is coarse-grained due to two main disadvantages. ❶ Within the axe target region, certain local areas exhibit relatively low association scores. ❷ Outside the axe region,

residual attention is present in areas where ideally no attention should be focused.

To this end, we propose to refine the attention map with a segmentation network to ensure better results in terms of accuracy and detail.

4.3.2 Architecture Design

The concept-guided segmentation module contains two submodules. As shown in Fig. 5, we use an attention extraction submodule to extract the coarse attention map first and then take it as the guidance input for the fine-grained segmentation submodule to output the final segmentation result. Both the submodules are classical U-Net architecture used in text-to-image models whose process takes multimodality input (refer to architecture [31]).

Specifically, given an image \mathbf{I} and its corresponding concept representation \mathbf{c}^* , the concept-guided segmentation module first transforms the image into a latent representation \mathbf{z} at time step t . Using this latent \mathbf{z}_t and concept representation \mathbf{c}^* as input, the attention extraction submodule generates an attention map following Eq. (6). Notably, the fine-grained segmentation submodule differs slightly from the traditional U-Net in text-to-image model by incorporating an additional cross-attention mechanism to process the attention map \mathbf{f}_{attn} as supplementary guidance alongside the prior guidance (*i.e.*, concept representation \mathbf{c}^*). With latent \mathbf{z}_t , concept representation \mathbf{c}^* , and attention map \mathbf{f}_{attn} as inputs, the fine-grained segmentation submodule (*i.e.*, function $\text{FineSeg}(\cdot)$) leverages these components to produce the final segmentation output,

$$\mathbf{S}' = \text{FineSeg}(\epsilon_\phi, \mathbf{z}_t, t, \mathbf{c}^*, \mathbf{f}_{attn}), \quad (8)$$

where ϵ_ϕ denotes the parameters in the module. Finally, we apply a predefined threshold value λ to \mathbf{S}' for final processing. In subsequent experiments, we discuss the impact of choosing different threshold values λ on the co-saliency object detection results. For each pixel s in \mathbf{S}' , the value satisfies the following condition:

$$\mathbf{S} = \begin{cases} 1, & \text{if } s \geq \lambda \\ 0, & \text{otherwise} \end{cases} \quad (9)$$

5. Experiment

5.1. Experimental Setup

Datasets. Our experiments on the clean datasets were conducted on Cosal2015 [45], CoSOD3k [8], and CoCA [52]. These three datasets contain 2015, 3316, and 1295 images of 50, 160, and 80 groups respectively. In terms of the corrupted datasets, we applied six types of corruption methods to the Cosal2015 dataset, specifically including frost, fog,

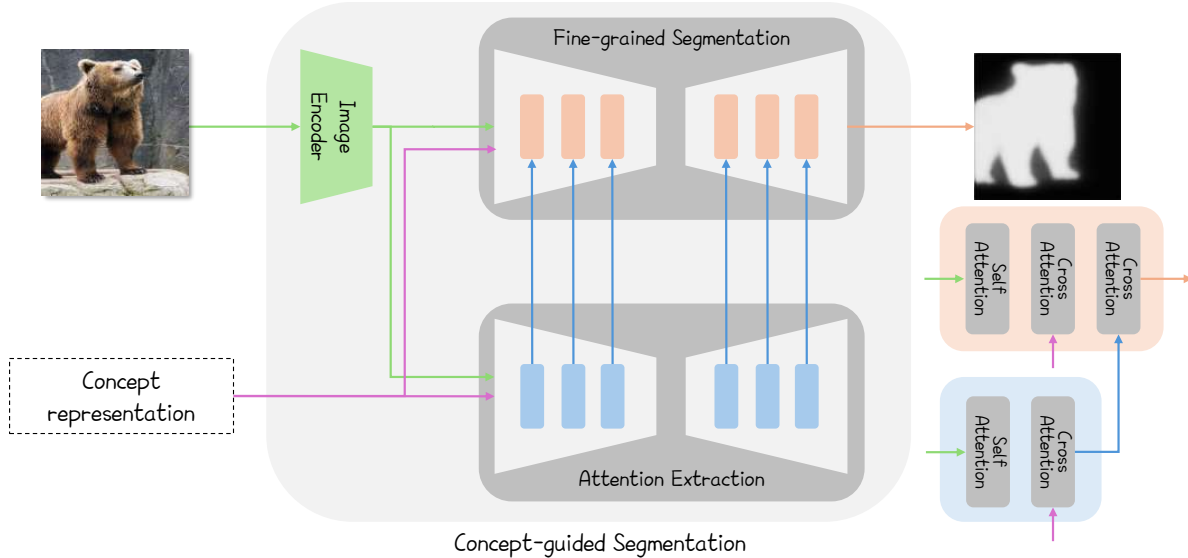


Figure 5. Concept-guided segmentation module.

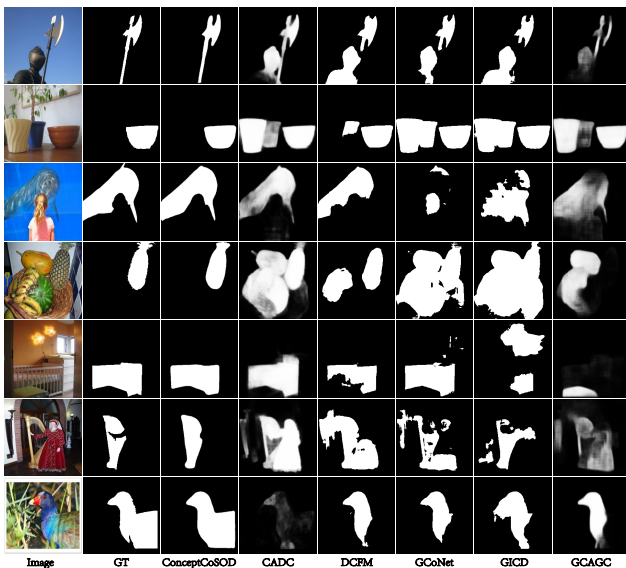


Figure 6. Visualization of our ConceptCoSOD method and other baselines on clean image dataset.

motion blur, defocus blur, and Gaussian noise from common corruption types [15], as well as the adversarial attack Jadena [13]. Specifically, we applied corruption to the first 50% of images in each image group while keeping the remaining 50% of images clean.

Baseline methods. We selected five comparison methods that have demonstrated excellent performance in co-saliency object detection, including GCAGC [48], GICD [51], GCoNet [9], DCFM [42] and CADC [50].

Metrics. We employ six metrics to evaluate co-salient ob-

Table 1. Co-saliency detection performance on clean datasets.

	Cosal2015					
	SR \uparrow	IoU \uparrow	MAE \downarrow	maxF \uparrow	$E_{\xi}^{max}\uparrow$	$S_m\uparrow$
GCAGC [48]	0.8029	0.7162	0.0813	0.8281	0.8888	0.8346
GICD [51]	0.8382	0.7484	0.0744	0.8261	0.8774	0.8314
GCoNet [9]	0.8272	0.7472	0.0708	0.8327	0.8808	0.8324
DCFM [42]	0.8486	0.7384	0.0678	0.8446	0.8883	0.8291
CADC [50]	0.8625	0.7723	0.0687	0.8550	0.8992	0.8591
CONCEPTCoSOD	0.8719	0.7556	0.0570	0.8292	0.8940	0.8385
	CoSOD3k					
	SR \uparrow	IoU \uparrow	MAE \downarrow	maxF \uparrow	$E_{\xi}^{max}\uparrow$	$S_m\uparrow$
GCAGC [48]	0.7026	0.6260	0.0929	0.7556	0.8518	0.7915
GICD [51]	0.7361	0.6564	0.0883	0.7461	0.8326	0.7779
GCoNet [9]	0.7322	0.6584	0.0773	0.7569	0.8464	0.7847
DCFM [42]	0.7677	0.6706	0.0712	0.7853	0.8645	0.7949
CADC [50]	0.7457	0.6737	0.0928	0.7644	0.8465	0.8052
CONCEPTCoSOD	0.8072	0.7003	0.0700	0.7853	0.8681	0.8070
	CoCA					
	SR \uparrow	IoU \uparrow	MAE \downarrow	maxF \uparrow	$E_{\xi}^{max}\uparrow$	$S_m\uparrow$
GCAGC [48]	0.3915	0.3766	0.1082	0.5086	0.7544	0.6684
GICD [51]	0.3683	0.4031	0.1455	0.4757	0.6778	0.6311
GCoNet [9]	0.3984	0.4206	0.1147	0.5089	0.7306	0.6517
DCFM [42]	0.4826	0.4697	0.0901	0.5697	0.7646	0.6914
CADC [50]	0.4239	0.4406	0.1339	0.5326	0.7370	0.6720
CONCEPTCoSOD	0.5644	0.5184	0.0956	0.5956	0.7593	0.7109

ject detection performance. Intersection over Union (IoU) assesses the overlap between the detected region and the ground truth, with the average IoU calculated across all detections. Detections with an IoU value above 0.5 are considered successful, and the success rate (SR) serves as an additional metric. Mean Absolute Error (MAE) [47] quantifies the average pixel-wise difference between the Co-SOD result and ground truth. Maximum F-measure (maxF) [1] calculates a harmonic mean of precision and recall, balancing these aspects in Co-SOD evaluations. The Enhanced Alignment Measure (E_{ξ}) [7] captures alignment and distribution by integrating pixel-level and image-level assessments. Lastly, the Structure Measure (S_m) [6] evaluates

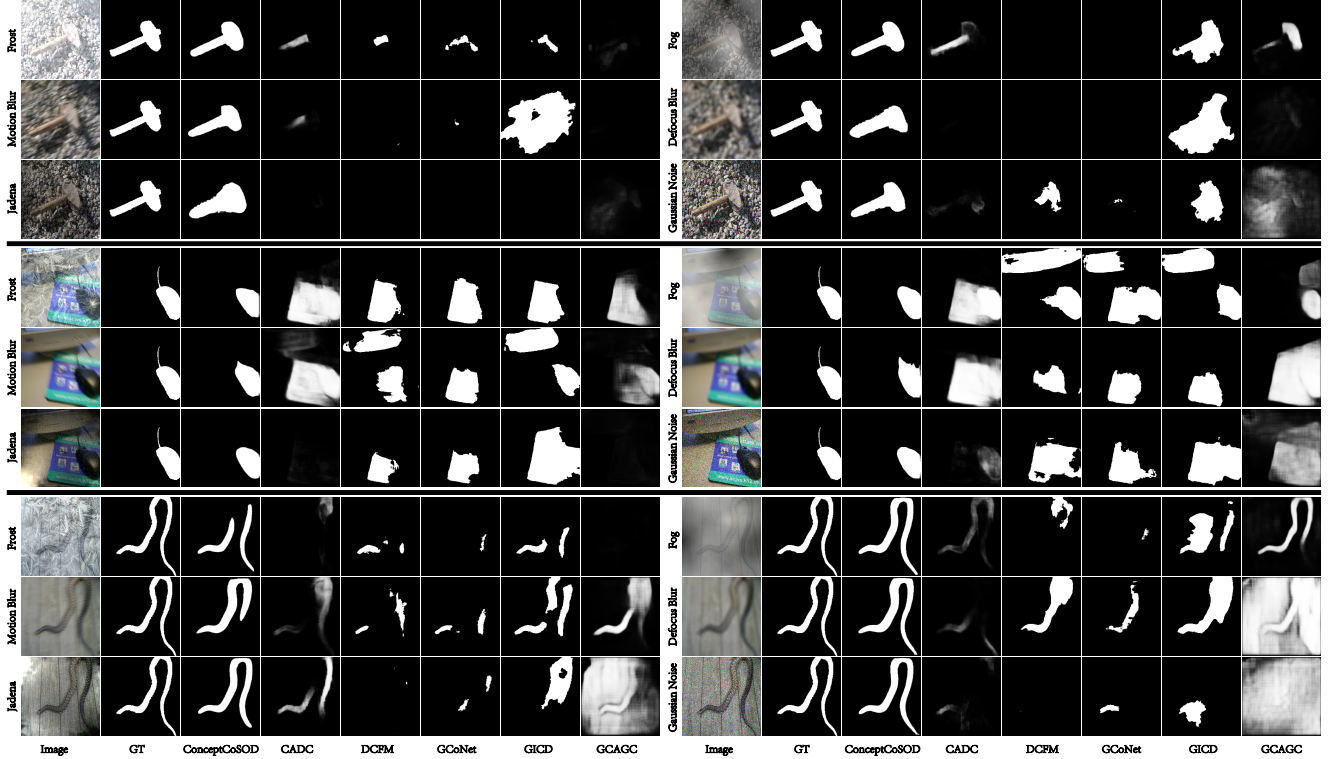


Figure 7. Visualization of our ConceptCoSOD method and other baselines on corrupted datasets.

Table 2. Results of our ConceptCoSOD method under different thresholds.

		threshold					
		0.3	0.4	0.5	0.6	0.7	0.8
Cosal2015	SR \uparrow	0.8540	0.8789	0.8719	0.8397	0.8000	0.7702
	IoU \uparrow	0.7057	0.7418	0.7556	0.7435	0.7083	0.6364
	MAE \downarrow	0.0810	0.0650	0.0570	0.0555	0.0600	0.0736
	maxF \uparrow	0.7788	0.8145	0.8292	0.8210	0.7934	0.7537
	$E_{\xi}^{max}\uparrow$	0.8713	0.8929	0.8940	0.8772	0.8483	0.8019
	$S_m\uparrow$	0.7976	0.8259	0.8385	0.8343	0.8164	0.7786
CoSOD3k	SR \uparrow	0.7587	0.7997	0.8072	0.7873	0.7358	0.6366
	IoU \uparrow	0.6484	0.6843	0.7003	0.6913	0.6481	0.5568
	MAE \downarrow	0.0993	0.0802	0.0700	0.0673	0.0718	0.0850
	maxF \uparrow	0.7263	0.7646	0.7853	0.7828	0.7551	0.6923
	$E_{\xi}^{max}\uparrow$	0.8351	0.8615	0.8681	0.8573	0.8285	0.7609
	$S_m\uparrow$	0.7625	0.7917	0.8070	0.8067	0.7858	0.7374
CoCA	SR \uparrow	0.5003	0.5467	0.5644	0.5528	0.5081	0.4162
	IoU \uparrow	0.4783	0.5072	0.5184	0.5012	0.4580	0.3758
	MAE \downarrow	0.1372	0.1117	0.0956	0.0844	0.0788	0.0779
	maxF \uparrow	0.5518	0.5823	0.5956	0.5819	0.5510	0.4869
	$E_{\xi}^{max}\uparrow$	0.7243	0.7496	0.7593	0.7441	0.7112	0.6390
	$S_m\uparrow$	0.6669	0.6952	0.7109	0.7090	0.6912	0.6522

structural similarities, considering both region-based and object-based coherence.

Implementation details. In the group-image concept learning module, the timestep t is set to 1,000. The learning rate for updating \mathbf{c}^* is set to $5e^{-4}$, and the max train step is set to 2,000. The threshold for segmentation is set to 0.5.

5.2. Comparison on Clean Datasets

We compare our ConceptCoSOD method with baselines on Cosal2015, CoSOD3k, and CoCA datasets. As shown in Table 1, the columns represent the baseline models and our method. The top two values for each metric are highlighted, with red indicating rank-1 and yellow indicating rank-2. For the Cosal2015 dataset, our method achieves five top-2 rankings, matching CADC’s performance. On the CoSOD3k dataset, our method attains rank-1 across all six metrics. For the CoCA dataset, our method secures six top-2 rankings, equivalent to DCFM. Overall, our method demonstrates the best performance across all three datasets.

5.3. Comparison on Corrupted Datasets

The robustness of our co-salient object detection method is essential, as real-world images often include various corruptions. To assess robustness, we applied common corruptions and an adversarial attack, as presented in Table 3. Specifically, we evaluated weather-related corruptions (frost, fog), common distortions (motion blur, defocus blur, Gaussian noise) [15], and an adversarial attack (Jadena) [13]. The top two scores for each metric are highlighted, with red indicating the highest and yellow indicating the second highest. Results show that our method achieves top performance under frost, motion blur, adver-

Table 3. Co-saliency detection performance on corrupted datasets.

	Frost						Fog					
	SR↑	IoU↑	MAE↓	maxF↑	$E_{\xi}^{max}\uparrow$	$S_m\uparrow$	SR↑	IoU↑	MAE↓	maxF↑	$E_{\xi}^{max}\uparrow$	$S_m\uparrow$
GCAGC [48]	0.6714	0.6114	0.1121	0.7548	0.8394	0.7769	0.7548	0.6725	0.0944	0.7944	0.8628	0.8089
GICD [51]	0.7315	0.6589	0.1008	0.7581	0.8256	0.7745	0.7736	0.6892	0.0935	0.7799	0.8443	0.7941
GCoNet [9]	0.6823	0.6196	0.1052	0.7380	0.8049	0.7539	0.7399	0.6697	0.0908	0.7729	0.8357	0.7865
DCFM [42]	0.6848	0.6093	0.1037	0.7462	0.8056	0.7482	0.7548	0.6618	0.0872	0.7879	0.8427	0.7826
CADC [50]	0.7429	0.6683	0.0956	0.7798	0.8469	0.8014	0.8029	0.7205	0.0822	0.8173	0.8734	0.8320
CONCEPTCoSOD	0.8074	0.7034	0.0837	0.7824	0.8524	0.7983	0.8367	0.7179	0.0760	0.7925	0.8676	0.8089
	Motion Blur						Defocus Blur					
	SR↑	IoU↑	MAE↓	maxF↑	$E_{\xi}^{max}\uparrow$	$S_m\uparrow$	SR↑	IoU↑	MAE↓	maxF↑	$E_{\xi}^{max}\uparrow$	$S_m\uparrow$
GCAGC [48]	0.6853	0.6113	0.1240	0.7394	0.8191	0.7700	0.7057	0.6269	0.1246	0.7464	0.8197	0.7747
GICD [51]	0.7052	0.6332	0.1088	0.7290	0.8117	0.7567	0.7126	0.6310	0.1059	0.7317	0.8090	0.7571
GCoNet [9]	0.6203	0.5678	0.1105	0.6935	0.7683	0.7247	0.5781	0.5320	0.1180	0.6578	0.7320	0.7038
DCFM [42]	0.6655	0.5948	0.0997	0.7287	0.7969	0.7404	0.6684	0.5958	0.0995	0.7352	0.7968	0.7422
CADC [50]	0.7260	0.6504	0.1026	0.7538	0.8345	0.7898	0.6928	0.6162	0.1054	0.7310	0.8252	0.7736
CONCEPTCoSOD	0.7895	0.6772	0.0868	0.7542	0.8403	0.7830	0.7464	0.6492	0.0939	0.7233	0.8087	0.7657
	Adversarial Attack (Jadana)						Gaussian Noise					
	SR↑	IoU↑	MAE↓	maxF↑	$E_{\xi}^{max}\uparrow$	$S_m\uparrow$	SR↑	IoU↑	MAE↓	maxF↑	$E_{\xi}^{max}\uparrow$	$S_m\uparrow$
GCAGC [48]	0.5980	0.5501	0.1444	0.6900	0.7837	0.7347	0.5320	0.5156	0.2265	0.6332	0.6912	0.6746
GICD [51]	0.6794	0.6162	0.1110	0.7111	0.7905	0.7481	0.6853	0.6288	0.1224	0.7200	0.7995	0.7470
GCoNet [9]	0.5627	0.5257	0.1178	0.6447	0.7218	0.7014	0.6054	0.5571	0.1183	0.6887	0.7663	0.7155
DCFM [42]	0.5995	0.5404	0.1097	0.6678	0.7412	0.7112	0.6312	0.5659	0.1112	0.7044	0.7760	0.7217
CADC [50]	0.7176	0.6417	0.0978	0.7553	0.8334	0.7886	0.7141	0.6457	0.1070	0.7553	0.8295	0.7852
CONCEPTCoSOD	0.8004	0.6947	0.0921	0.7722	0.8413	0.7907	0.7756	0.6801	0.0897	0.7584	0.8282	0.7858

sarial attacks, Gaussian noise, and defocus blur. For fog corruption, our method performs slightly below CADC but remains highly competitive. Overall, our method demonstrates superior robustness across a variety of corruptions.

5.4. Visualization

As shown in Fig. 6, we demonstrate the visualization result comparison between our method and baselines. Our method demonstrates precise segmentation of the target object, closely resembling the ground truth. In contrast, the baseline results are less accurate, often exhibiting incomplete segmentation of the target object or including non-target objects within the segmentation area.

As shown in Fig. 7, we demonstrate the visualization result comparison between our method and baselines under corruptions. There are three cases, each containing six types of corruption. In most instances, only our ConceptCoSOD method effectively segments the target object, while other methods largely fail to identify it. This outcome demonstrates the superior robustness of our method against corruption compared to others.

5.5. Ablation Study

Threshold. In the Co-SOD task, the threshold for generating the final binary map is a key hyperparameter. To assess its influence, as shown in Table 2, we evaluate the results across a threshold range of [0.3, 0.8]. The dataset names are listed in the first column, with metrics in the second column and threshold values in the second row. Results indicate that threshold values of 0.5 provide optimal performance across

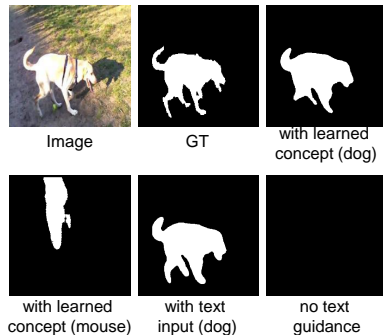


Figure 8. Ablation on concept guidance.

six metrics. Therefore, we select 0.5 as the default threshold value for our experiments.

Concept guidance. We utilize different concepts (text embeddings) to assess their influence on segmentation performance. As shown in Fig. 8, the input image is of the dog concept. We observe that segmentation using the concept learned from the dog image group achieves better results in segmenting the dog object compared to the concept learned from the mouse image group. Also, if we directly put the text embedding of the word “dog” as guidance, the segmentation result is good, reflecting the effect of text semantics as supplementary information. If we do not put any text as guidance, the result is black, which is totally wrong.

5.6. Limitation

According to the robustness analysis, our method does not yet outperform other Co-SOD approaches comprehen-

sively. In future work, we aim to enhance the robustness through advanced data augmentation techniques.

6. Conclusion

This paper presents a novel approach, ConceptCoSOD, which leverages text-based semantic guidance for co-salient object detection (Co-SOD). Unlike traditional Co-SOD methods that rely solely on image-based features, ConceptCoSOD introduces a robust (image-text)-to-image framework, enhancing object segmentation accuracy by incorporating semantic information from text. This approach not only mitigates the challenges posed by inter-object variations and background noise but also showcases the potential of integrating text-driven semantics into Co-SOD tasks, providing a new direction for future research in vision-language models for complex segmentation tasks. In future work, we aim to enhance the robustness of concept learning to improve the method’s practicality.

References

- [1] Radhakrishna Achanta, Sheila Hemami, Francisco Estrada, and Sabine Susstrunk. Frequency-tuned salient region detection. In *2009 IEEE conference on computer vision and pattern recognition*, pages 1597–1604. IEEE, 2009.
- [2] Luca Barsellotti, Roberto Amoroso, Marcella Cornia, Lorenzo Baraldi, and Rita Cucchiara. Training-free open-vocabulary segmentation with offline diffusion-augmented prototype generation. In *Proceedings of the IEEE/CVF Conference on Computer Vision and Pattern Recognition*, pages 3689–3698, 2024.
- [3] Kai-Yueh Chang, Tyng-Luh Liu, and Shang-Hong Lai. From co-saliency to co-segmentation: An efficient and fully unsupervised energy minimization model. In *CVPR 2011*, pages 2129–2136. IEEE, 2011.
- [4] Florinel-Alin Croitoru, Vlad Hondru, Radu Tudor Ionescu, and Mubarak Shah. Diffusion models in vision: A survey. *IEEE Transactions on Pattern Analysis and Machine Intelligence*, 2023.
- [5] Giannis Daras and Alexandros G Dimakis. Multiresolution textual inversion. *arXiv preprint arXiv:2211.17115*, 2022.
- [6] Deng-Ping Fan, Ming-Ming Cheng, Yun Liu, Tao Li, and Ali Borji. Structure-measure: A new way to evaluate foreground maps. In *Proceedings of the IEEE international conference on computer vision*, pages 4548–4557, 2017.
- [7] Deng-Ping Fan, Cheng Gong, Yang Cao, Bo Ren, Ming-Ming Cheng, and Ali Borji. Enhanced-alignment measure for binary foreground map evaluation. *arXiv preprint arXiv:1805.10421*, 2018.
- [8] Deng-Ping Fan, Zheng Lin, Ge-Peng Ji, Dingwen Zhang, Huazhu Fu, and Ming-Ming Cheng. Taking a deeper look at co-salient object detection. In *Proceedings of the IEEE/CVF conference on computer vision and pattern recognition*, pages 2919–2929, 2020.
- [9] Qi Fan, Deng-Ping Fan, Huazhu Fu, Chi-Keung Tang, Ling Shao, and Yu-Wing Tai. Group collaborative learning for co-salient object detection. In *Proceedings of the IEEE/CVF Conference on Computer Vision and Pattern Recognition*, pages 12288–12298, 2021.
- [10] Huazhu Fu, Xiaochun Cao, and Zhuowen Tu. Cluster-based co-saliency detection. *IEEE Transactions on Image Processing*, 22(10):3766–3778, 2013.
- [11] Rinon Gal, Yuval Alaluf, Yuval Atzmon, Patashnik, Amit Haim Bermano, Gal Chechik, and Daniel Cohen-or. An image is worth one word: Personalizing text-to-image generation using textual inversion. In *The Eleventh International Conference on Learning Representations*, 2023.
- [12] Rinon Gal, Moab Arar, Yuval Atzmon, Amit H Bermano, Gal Chechik, and Daniel Cohen-Or. Designing an encoder for fast personalization of text-to-image models. *arXiv preprint arXiv:2302.12228*, 2023.
- [13] Ruijun Gao, Qing Guo, Felix Juefei-Xu, Hongkai Yu, Huazhu Fu, Wei Feng, Yang Liu, and Song Wang. Can you spot the chameleon? adversarially camouflaging images from co-salient object detection. In *Proceedings of the IEEE/CVF Conference on Computer Vision and Pattern Recognition*, pages 2150–2159, 2022.
- [14] Junwei Han, Gong Cheng, Zhenpeng Li, and Dingwen Zhang. A unified metric learning-based framework for co-saliency detection. *IEEE Transactions on Circuits and Systems for Video Technology*, 28(10):2473–2483, 2017.
- [15] Dan Hendrycks and Thomas Dietterich. Benchmarking neural network robustness to common corruptions and perturbations. *Proceedings of the International Conference on Learning Representations*, 2019.
- [16] Jonathan Ho, Ajay Jain, and Pieter Abbeel. Denoising diffusion probabilistic models. *Advances in neural information processing systems*, 33:6840–6851, 2020.
- [17] Kuang-Jui Hsu, Chung-Chi Tsai, Yen-Yu Lin, Xiaoning Qian, and Yung-Yu Chuang. Unsupervised cnn-based co-saliency detection with graphical optimization. In *Proceedings of the European conference on computer vision (ECCV)*, pages 485–501, 2018.
- [18] Edward J Hu, Yelong Shen, Phillip Wallis, Zeyuan Allen-Zhu, Yuanzhi Li, Shean Wang, Lu Wang, and Weizhu Chen. Lora: Low-rank adaptation of large language models. *arXiv preprint arXiv:2106.09685*, 2021.
- [19] Yihao Huang, Felix Juefei-Xu, Qing Guo, Jie Zhang, Yutong Wu, Ming Hu, Tianlin Li, Geguang Pu, and Yang Liu. Personalization as a shortcut for few-shot backdoor attack against text-to-image diffusion models. In *Proceedings of the AAAI Conference on Artificial Intelligence*, pages 21169–21178, 2024.
- [20] Yihao Huang, Le Liang, Tianlin Li, Xiaojun Jia, Run Wang, Weikai Miao, Geguang Pu, and Yang Liu. Perception-guided jailbreak against text-to-image models. *arXiv preprint arXiv:2408.10848*, 2024.
- [21] Koteswar Rao Jerripothula, Jianfei Cai, and Junsong Yuan. Cats: Co-saliency activated tracklet selection for video co-localization. In *Computer Vision—ECCV 2016: 14th European Conference, Amsterdam, The Netherlands, October 11–14, 2016, Proceedings, Part VII 14*, pages 187–202. Springer, 2016.

- [22] Koteswar Rao Jerripothula, Jianfei Cai, and Junsong Yuan. Efficient video object co-localization with co-saliency activated tracklets. *IEEE Transactions on Circuits and Systems for Video Technology*, 29(3):744–755, 2018.
- [23] Bo Jiang, Xingyue Jiang, Ajian Zhou, Jin Tang, and Bin Luo. A unified multiple graph learning and convolutional network model for co-saliency estimation. In *Proceedings of the 27th ACM international conference on multimedia*, pages 1375–1382, 2019.
- [24] Wen-Da Jin, Jun Xu, Ming-Ming Cheng, Yi Zhang, and Wei Guo. Icnct: Intra-saliency correlation network for co-saliency detection. *Advances in Neural Information Processing Systems*, 33:18749–18759, 2020.
- [25] Tero Karras, Timo Aila, Samuli Laine, and Jaakko Lehtinen. Progressive growing of GANs for improved quality, stability, and variation. In *International Conference on Learning Representations*, 2018.
- [26] Bo Li, Zhengxing Sun, Lv Tang, Yunhan Sun, and Jinlong Shi. Detecting robust co-saliency with recurrent co-attention neural network. In *IJCAI*, page 6, 2019.
- [27] Hongliang Li and King Ngi Ngan. A co-saliency model of image pairs. *IEEE Transactions on Image Processing*, 20(12):3365–3375, 2011.
- [28] Hongliang Li, Fanman Meng, and King Ngi Ngan. Co-salient object detection from multiple images. *IEEE Transactions on Multimedia*, 15(8):1896–1909, 2013.
- [29] Ziyi Li, Qinye Zhou, Xiaoyun Zhang, Ya Zhang, Yanfeng Wang, and Weidi Xie. Open-vocabulary object segmentation with diffusion models. In *Proceedings of the IEEE/CVF International Conference on Computer Vision*, pages 7667–7676, 2023.
- [30] Koutilya Pnvr, Bharat Singh, Pallabi Ghosh, Behjat Siddique, and David Jacobs. Ld-znet: A latent diffusion approach for text-based image segmentation. In *Proceedings of the IEEE/CVF International Conference on Computer Vision*, pages 4157–4168, 2023.
- [31] Robin Rombach, Andreas Blattmann, Dominik Lorenz, Patrick Esser, and Björn Ommer. High-resolution image synthesis with latent diffusion models. In *Proceedings of the IEEE/CVF Conference on Computer Vision and Pattern Recognition*, pages 10684–10695, 2022.
- [32] Nataniel Ruiz, Yuanzhen Li, Varun Jampani, Yael Pritch, Michael Rubinstein, and Kfir Aberman. Dreambooth: Fine tuning text-to-image diffusion models for subject-driven generation. *arXiv preprint arXiv:2208.12242*, 2022.
- [33] Jing Shi, Wei Xiong, Zhe Lin, and Hyun Joon Jung. Instant-booth: Personalized text-to-image generation without test-time finetuning. *arXiv preprint arXiv:2304.03411*, 2023.
- [34] Hangke Song, Zhi Liu, Yufeng Xie, Lishan Wu, and Mengke Huang. Rgb-d co-saliency detection via bagging-based clustering. *IEEE Signal Processing Letters*, 23(12):1722–1726, 2016.
- [35] stability ai. Stable diffusion. <https://stability.ai/>, 2024.
- [36] Jiapeng Tang, Dan Xu, Xin Zuo, and Qiang Qian. Co-saliency detection based on feature enhancement and contrast learning. In *2024 5th International Seminar on Artificial Intelligence, Networking and Information Technology (AINIT)*, pages 2292–2300. IEEE, 2024.
- [37] Raphael Tang, Linqing Liu, Akshat Pandey, Zhiying Jiang, Gefei Yang, Karun Kumar, Pontus Stenetorp, Jimmy Lin, and Ferhan Ture. What the daam: Interpreting stable diffusion using cross attention. *arXiv preprint arXiv:2210.04885*, 2022.
- [38] Wenguan Wang, Jianbing Shen, and Fatih Porikli. Saliency-aware geodesic video object segmentation. In *Proceedings of the IEEE conference on computer vision and pattern recognition*, pages 3395–3402, 2015.
- [39] Lina Wei, Shanshan Zhao, Omar El Farouk Bourahla, Xi Li, Fei Wu, and Yueting Zhuang. Deep group-wise fully convolutional network for co-saliency detection with graph propagation. *IEEE Transactions on Image Processing*, 28(10):5052–5063, 2019.
- [40] Weijia Wu, Yuzhong Zhao, Mike Zheng Shou, Hong Zhou, and Chunhua Shen. Diffumask: Synthesizing images with pixel-level annotations for semantic segmentation using diffusion models. In *Proceedings of the IEEE/CVF International Conference on Computer Vision*, pages 1206–1217, 2023.
- [41] Jiarui Xu, Sifei Liu, Arash Vahdat, Wonmin Byeon, Xiaolong Wang, and Shalini De Mello. Open-vocabulary panoptic segmentation with text-to-image diffusion models. In *Proceedings of the IEEE/CVF Conference on Computer Vision and Pattern Recognition*, pages 2955–2966, 2023.
- [42] Siyue Yu, Jimin Xiao, Bingfeng Zhang, and Eng Gee Lim. Democracy does matter: Comprehensive feature mining for co-salient object detection. In *Proceedings of the IEEE/CVF Conference on Computer Vision and Pattern Recognition*, pages 979–988, 2022.
- [43] Yu Zeng, Yunzhi Zhuge, Huchuan Lu, and Lihe Zhang. Joint learning of saliency detection and weakly supervised semantic segmentation. In *Proceedings of the IEEE/CVF international conference on computer vision*, pages 7223–7233, 2019.
- [44] Chenshuang Zhang, Chaoning Zhang, Mengchun Zhang, and In So Kweon. Text-to-image diffusion model in generative ai: A survey. *arXiv preprint arXiv:2303.07909*, 2023.
- [45] Dingwen Zhang, Junwei Han, Chao Li, Jingdong Wang, and Xuelong Li. Detection of co-salient objects by looking deep and wide. *International Journal of Computer Vision*, 120:215–232, 2016.
- [46] Dingwen Zhang, Deyu Meng, and Junwei Han. Co-saliency detection via a self-paced multiple-instance learning framework. *IEEE transactions on pattern analysis and machine intelligence*, 39(5):865–878, 2016.
- [47] Dingwen Zhang, Huazhu Fu, Junwei Han, Ali Borji, and Xuelong Li. A review of co-saliency detection algorithms: Fundamentals, applications, and challenges. *ACM Transactions on Intelligent Systems and Technology (TIST)*, 9(4):1–31, 2018.
- [48] Kaihua Zhang, Tengpeng Li, Shiwen Shen, Bo Liu, Jin Chen, and Qingshan Liu. Adaptive graph convolutional network with attention graph clustering for co-saliency detection. In *Proceedings of the IEEE/CVF conference on computer vision and pattern recognition*, pages 9050–9059, 2020.

- [49] Kaihua Zhang, Mingliang Dong, Bo Liu, Xiao-Tong Yuan, and Qingshan Liu. Deepacg: Co-saliency detection via semantic-aware contrast gromov-wasserstein distance. In *Proceedings of the IEEE/CVF Conference on Computer Vision and Pattern Recognition*, pages 13703–13712, 2021.
- [50] Ni Zhang, Junwei Han, Nian Liu, and Ling Shao. Summarize and search: Learning consensus-aware dynamic convolution for co-saliency detection. In *Proceedings of the IEEE/CVF International Conference on Computer Vision*, pages 4167–4176, 2021.
- [51] Zhao Zhang, Wenda Jin, Jun Xu, and Ming-Ming Cheng. Gradient-induced co-saliency detection. In *Computer Vision—ECCV 2020: 16th European Conference, Glasgow, UK, August 23–28, 2020, Proceedings, Part XII 16*, pages 455–472. Springer, 2020.
- [52] Jia-Xing Zhao, Jiang-Jiang Liu, Deng-Ping Fan, Yang Cao, Jufeng Yang, and Ming-Ming Cheng. Egnnet: Edge guidance network for salient object detection. In *Proceedings of the IEEE/CVF international conference on computer vision*, pages 8779–8788, 2019.
- [53] Xiaoju Zheng, Zheng-Jun Zha, and Liansheng Zhuang. A feature-adaptive semi-supervised framework for co-saliency detection. In *Proceedings of the 26th ACM international conference on Multimedia*, pages 959–966, 2018.